

Superconducting single-phase $\text{Sr}_{1-x}\text{La}_x\text{CuO}_2$ thin films with improved crystallinity grown by pulsed laser deposition

Victor Leca,^{a)} Dave H. A. Blank, and Guus RijndersMESA⁺ Institute for Nanotechnology, Faculty of Science and Technology, University of Twente, 7500 AE Enschede, The Netherlands

Sara Bals and Gustaaf van Tendeloo

EMAT, University of Antwerp, Groenenborgerlaan 171, B-2020 Antwerp, Belgium

(Received 10 February 2006; accepted 19 July 2006; published online 31 August 2006)

$\text{Sr}_{1-x}\text{La}_x\text{CuO}_{2-\delta}$ ($x=0.10-0.20$) thin films exhibiting an oxygen-deficient $2\sqrt{2}a_p \times 2\sqrt{2}a_p \times c$ structure (a_p and c represent the cell parameters of the perovskite subcell) were epitaxially grown by means of pulsed laser deposition in low-pressure oxygen ambient. (001) KTaO_3 and (001) SrTiO_3 single crystals were used as substrates, with BaTiO_3 as buffer layer. The $\text{Sr}_{1-x}\text{La}_x\text{CuO}_{2-\delta}$ films were oxidized during cooling down in order to yield the infinite-layer-type structure. By applying this method, high quality single-phase $\text{Sr}_{1-x}\text{La}_x\text{CuO}_2$ thin films could be obtained for $0.10 \leq x \leq 0.175$ doping range. The films grown on $\text{BaTiO}_3/\text{KTaO}_3$ show superconductivity for $0.15 \leq x \leq 0.175$ with optimum doping at $x=0.15$, in contrast with previously reported data. © 2006 American Institute of Physics. [DOI: 10.1063/1.2339840]

The infinite-layer (IL) $\text{Sr}_{1-x}\text{Ln}_x\text{CuO}_2$ ($\text{Ln}=\text{La, Nd, Pr, Ga}$) compounds exhibit n -type superconductivity with a maximum $T_c \sim 43$ K.¹⁻³ A solubility limit smaller than $x=0.15$ was found both in bulk samples¹⁻³ and in thin films.⁴⁻⁶ Magnetic measurements on bulk samples showed that T_c^{onset} remains constant for any doping concentration in the range $0.05 < x \leq 0.12$, while the Meissner fraction increases with x , showing a maximum for $x=0.10$.^{2,3} The decrease of the Meissner signal for $x > 0.10$ is associated with the impurity phases formed due to (low) solubility limit of Ln.¹⁻³ The low solubility limit is considered the reason for the shift of the optimum doping to lower values (i.e., $x \sim 0.10$) and not at the expected 0.15 electrons/ CuO_2 .⁷ Therefore, the upper limit for Ln doping in single-phase samples for which superconductivity can be observed has not been identified. In this perspective, it is important to find methods for yielding single-phase IL-type $\text{Sr}_{1-x}\text{Ln}_x\text{CuO}_2$ samples, mainly in the $x > 0.10$ region.

One of the secondary phases observed in $\text{Sr}_{1-x}\text{Ln}_x\text{CuO}_2$ systems is the $2\sqrt{2}a_p \times 2\sqrt{2}a_p \times c$ modulated (super)structure, where a_p and c refer to the perovskite subcell parameters.^{4,8} Mercey *et al.*⁸ have shown that this phase forms due to ordering of the Sr and Ln atoms, as well as of the oxygen atoms and vacancies. We have previously shown that $\text{Sr}_{0.85}\text{La}_{0.15}\text{CuO}_{2-\delta}$ thin films exhibiting only the $2\sqrt{2}a_p \times 2\sqrt{2}a_p \times c$ structure can be epitaxially stabilized on SrTiO_3 substrates by means of pulsed laser deposition (PLD).^{9,10} According to x-ray diffraction (XRD) and high-resolution transmission electron microscopy (HRTEM) data, the modulated structure formed over a wide composition range, $0.10 \leq x \leq 0.20$. This was achieved by using relatively low oxygen partial pressure (e.g., 10^{-2} mbar O_2) during growth followed by cooling down in nitrogen (1 bar). In Fig. 1 cross section HRTEM [Fig. 1(a)] and corresponding electron diffraction (ED) micrograph of the [010] plane [Fig. 1(b)] as well as plan view HRTEM [Fig. 1(c)] and corresponding ED pattern

of the [001] plane [Fig. 1(d)] of a single-phase $\text{Sr}_{0.85}\text{La}_{0.15}\text{CuO}_{2-\delta}$ thin film exhibiting the $2\sqrt{2}a_p \times 2\sqrt{2}a_p \times c$ structure are shown. The in-plane lattice constants of these oxygen-deficient $\text{Sr}_{1-x}\text{La}_x\text{CuO}_{2-\delta}$ films closely match the ones of the substrate.^{9,10} The ability of this structure to match the in-plane cell parameters of the substrate may be used to obtain films with reduced strain during growth, therefore avoiding the formation of secondary phases. The questions we try to answer here are if this oxygen-deficient structure can be used as an intermediate phase in yielding single-

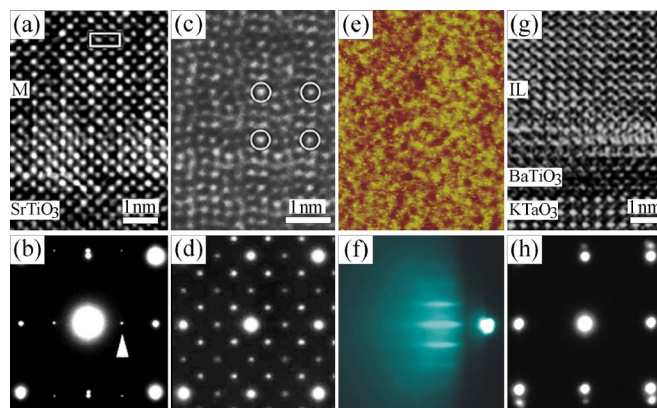


FIG. 1. (Color online) [(a)–(d)] Structural data of single-phase $\text{Sr}_{0.85}\text{La}_{0.15}\text{CuO}_{2-\delta}$ thin film grown on SrTiO_3 showing the $2\sqrt{2}a_p \times 2\sqrt{2}a_p \times c$ modulated structure: (a) cross section HRTEM image and (b) corresponding [010] ED pattern. In (a) the modulated structure, marked M and indicated by a white rectangle, appears as a doubling of a_p , whereas the arrow in (b) indicates a diffraction spot that is due to the modulated structure. (c) Plan view HRTEM image and (d) corresponding [001] ED pattern. The white circles in (c) indicate the size of the $2\sqrt{2}a_p \times 2\sqrt{2}a_p$ unit cell. The bright spots in (d) correspond to the perovskite lattice parameters (a_p), whereas the weaker spots are due to the modulated structure. [(e)–(h)] Morphological and structural data of a single-phase $\text{Sr}_{0.85}\text{La}_{0.15}\text{CuO}_2$ thin film grown on $\text{BaTiO}_3/\text{KTaO}_3$: (e) AFM image ($1.5 \times 2 \mu\text{m}^2$, rms ~ 0.5 nm) and (f) RHEED pattern recorded at 10^{-3} mbar O_2 and 550°C with [100] beam azimuth. (g) Cross section HRTEM image and (h) corresponding [010] ED pattern showing an IL-type structure. The smaller spots in (h) correspond to the (001) plane of the film.

^{a)}Electronic mail: victor.leca@uni-tuebingen.de

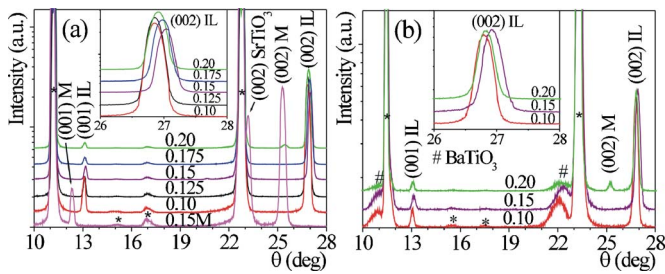


FIG. 2. (Color online) XRD θ - 2θ patterns of $\text{Sr}_{1-x}\text{La}_x\text{CuO}_{2-\delta}$ ($x = 0.10$ – 0.20) thin films grown on (a) $\text{BaTiO}_3/\text{KTaO}_3$ and (b) $\text{BaTiO}_3/\text{SrTiO}_3$. The diffraction peaks corresponding to the substrate are marked with an asterisk; M marks the $2\sqrt{2}a_p \times 2\sqrt{2}a_p \times c$ phase.

phase $\text{Sr}_{1-x}\text{La}_x\text{CuO}_2$ films and, furthermore, what are the implications on the morphological, structural, and electrical properties of the resulting films. In order to obtain the superconductive phase in $\text{Sr}_{1-x}\text{Ln}_x\text{CuO}_2$ thin films, a postdeposition reduction step that removes the apex oxygen from the Sr–O layers is generally used.^{4–6} In this letter, however, we present a synthesis method that requires oxygenation during sample cooling in order to yield superconductivity in $\text{Sr}_{1-x}\text{Ln}_x\text{CuO}_2$ thin films, with $\text{Ln}=\text{La}$.

Oxygen-deficient 75–140 nm thick $\text{Sr}_{1-x}\text{La}_x\text{CuO}_{2-\delta}$ ($x = 0.10$ – 0.20) films having a $2\sqrt{2}a_p \times 2\sqrt{2}a_p \times c$ ordered structure were grown by means of PLD using a KrF excimer laser ($\lambda = 248$ nm).¹¹ A substrate temperature of 550 °C and a background pressure of $(0.5$ – $1) \times 10^{-3}$ mbar O_2 were used for deposition.^{9,10} The films were grown mainly on (001) KTaO_3 ;⁶ however, in order to study the role of the strain induced by the substrate on the film properties, some films were also deposited on (001) SrTiO_3 . BaTiO_3 (with thickness of ~ 4 nm on KTaO_3 and ~ 20 nm on SrTiO_3 , respectively) was used as buffer layer.^{10,12} Only few unit cells of BaTiO_3 are deposited on KTaO_3 so that the buffer layer is coherent with the substrate and, therefore, fully strained. When deposited on SrTiO_3 , the BaTiO_3 layer was used to induce tensile strain in the $\text{Sr}_{1-x}\text{La}_x\text{CuO}_2$ films with the aim of increasing their stability.¹³ In case of KTaO_3 , the buffer layer helped to improve the surface morphology of the substrate.¹⁰ After growth the $\text{Sr}_{1-x}\text{La}_x\text{CuO}_{2-\delta}$ films were oxidized during cooling down to ~ 430 °C (with a rate of 7.5 °C/min) inside the deposition chamber while keeping the pressure used during deposition. After reaching this temperature, the samples were placed in the loadlock for faster cooling to room temperature. A longer oxygen diffusion time resulted in lack of superconductivity in the (optimally doped) films most probably due to inclusion of interstitial oxygen. The cation composition of the films has been measured by means of x-ray fluorescence (XRF). These measurements confirmed the stoichiometric deposition except for a small Sr deficiency (up to 7.5%) in some $\text{Sr}_{1-x}\text{La}_x\text{CuO}_2$ films grown on $\text{BaTiO}_3/\text{SrTiO}_3$.

In Fig. 1 typical atomic force microscopy (AFM) image [Fig. 1(e)] and high-pressure reflection high-energy electron diffraction (RHEED) pattern [Fig. 1(f)] for a $\text{Sr}_{0.85}\text{La}_{0.15}\text{CuO}_2$ film grown on $\text{BaTiO}_3/\text{KTaO}_3$ are shown. The streaky RHEED patterns observed during growth showed that the films have a smooth surface morphology, which was confirmed by AFM. XRD data showed that the $\text{Sr}_{1-x}\text{La}_x\text{CuO}_2$ films grown on either $\text{BaTiO}_3/\text{KTaO}_3$ [Fig. 2(a)] or $\text{BaTiO}_3/\text{SrTiO}_3$ [Fig. 2(b)] are single phase for $0.1 \leq x \leq 0.175$ and have a tetragonal IL-type structure. The films are c -axis oriented and well crystallized with narrow diffraction lines for all studied doping levels. An XRD pattern for an as-deposited $x=0.15$ film, with the modulated structure, is shown in Fig. 2(a) (marked 0.15 M). To obtain this structure, the film was covered *in situ* with a SrTiO_3 layer and then fast cooled down in order to quench the oxygen network. The stability of this modulated structure increases with x . The unit-cell parameters (calculated from XRD data) of the as-deposited films were determined to be $a_p \sim 3.97$ – 3.99 Å and $c \sim 3.53$ – 3.60 Å, on $\text{BaTiO}_3/\text{KTaO}_3$, and $a_p \sim 3.95$ – 3.97 Å and $c \sim 3.58$ – 3.62 Å, on $\text{BaTiO}_3/\text{SrTiO}_3$, respectively. The cell-parameter values depend on the actual oxygen and La content of the samples. After oxidation, the $\text{Sr}_{1-x}\text{La}_x\text{CuO}_2$ films grown on $\text{BaTiO}_3/\text{KTaO}_3$ have smaller lattice constants (both a and c axes) compared to those for the corresponding as-deposited films, due to incorporation of oxygen in the structure. However, for the films grown on $\text{BaTiO}_3/\text{SrTiO}_3$, the a axis is expanded while the c axis shrunk after the oxidation step. In case of SrTiO_3 , the use of BaTiO_3 as buffer layer results in a tensile strain in the $\text{Sr}_{1-x}\text{La}_x\text{CuO}_2$ films that stretches the Cu–O bonds, increasing the in-plane lattice parameter of the IL films. The evolution of the unit-cell parameters with $\text{La}(x)$ for $\text{Sr}_{1-x}\text{La}_x\text{CuO}_{2-\delta}$ films grown on $\text{BaTiO}_3/\text{KTaO}_3$ is presented in Table I. The films showing superconductivity have an in-plane lattice parameter close to $a \sim 3.98$ Å. The c -axis cell parameter of the films shows a minimum for $x=0.15$.

Small amounts of the modulated structure were observed in the $0.175 < x \leq 0.20$ $\text{Sr}_{1-x}\text{La}_x\text{CuO}_2$ films due to incomplete oxygenation during cooling, as shown by the XRD patterns in Figs. 2(a) and 2(b) for $x=0.20$ films. Probably the conversion of the modulated structure into the IL type is hampered for higher values of x . The concentration of the modulated structure increases with x in the $0.175 < x \leq 0.20$ range, but even for these doping levels the IL is the main phase present in the films. The increased stability of the IL structure in terms of La doping can be explained by the combined effect of (a) the selected buffer layer (in case of deposition on SrTiO_3) or of the KTaO_3 substrate with in-plane cell parameters that fit well those of the $\text{Sr}_{1-x}\text{La}_x\text{CuO}_2$ films⁶ and (b) by the use of the oxygen-deficient structure as intermediate phase. This reduces the possibility of nucleation of secondary phases such as $(\text{Sr}, \text{La})_{14}\text{Cu}_{24}\text{O}_{41-\delta}$.⁹ Compositional inhomogeneity is therefore avoided, as the secondary phase in the

TABLE I. Averaged XRD cell parameters of $\text{Sr}_{1-x}\text{La}_x\text{CuO}_{2-\delta}$ ($0.10 \leq x \leq 0.20$) thin films grown on $\text{BaTiO}_3/\text{KTaO}_3$. $x=0.15_M$ refers to the as-deposited $x=0.15$ film with $2\sqrt{2}a_p \times 2\sqrt{2}a_p \times c$ modulated structure.

| x | 0.10 | 0.125 | 0.15 | 0.175 | 0.20 | 0.15 _M |
|---------|-------|-------|-------|-------|-------|-------------------------|
| a (Å) | 3.965 | 3.968 | 3.978 | 3.981 | 3.987 | $2\sqrt{2} \times 3.99$ |
| c (Å) | 3.412 | 3.408 | 3.398 | 3.402 | 3.407 | 3.59 |

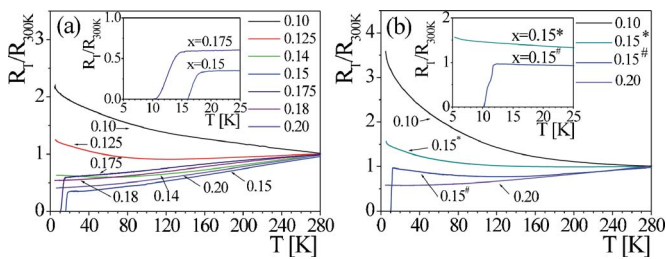


FIG. 3. (Color online) Temperature dependence of normalized resistance ($R_T/R_{300\text{K}}$) for $\text{Sr}_{1-x}\text{La}_x\text{CuO}_2$ thin films with different La contents grown on (a) $\text{BaTiO}_3/\text{KTaO}_3$ and (b) $\text{BaTiO}_3/\text{SrTiO}_3$. The thickness of the BaTiO_3 layer on SrTiO_3 was ~ 20 nm, with postdeposition annealing at 900°C and 5×10^{-7} mbar. Annealing times were 0.5 h for $x=0.10$, $0.15^\#$, and 0.20 films and 2 h for the $x=0.15^\#$ film, respectively.

$0.175 < x \leq 0.20$ films contains oxygen vacancies but no cation deficiency.

In Fig. 1 a cross section HRTEM image [Fig. 1(g)] and corresponding ED pattern along the [010] plane [Fig. 1(h)] are given for a $\text{Sr}_{0.85}\text{La}_{0.15}\text{CuO}_2$ film grown on $\text{BaTiO}_3/\text{KTaO}_3$. The film shows a single domain perovskite-type structure. No secondary phases were detected for this optimum oxidized $x=0.15$ sample, confirming the complete conversion of the as-deposited oxygen-deficient ordered structure to the IL-type structure during cooling.

The electrical properties (four-probe dc resistance) of the $\text{Sr}_{1-x}\text{La}_x\text{CuO}_2$ films as a function of La composition are presented in Fig. 3. The $0.1 \leq x \leq 0.125$ films grown on $\text{BaTiO}_3/\text{KTaO}_3$ showed semiconducting behavior, while for $0.125 < x < 0.15$ films a semimetal-like behavior was observed [see Fig. 3(a)]. Superconductivity was observed in a relatively narrow doping range, $0.15 \leq x \leq 0.175$, with a maximum $T_c \sim 16$ K for $x=0.15$ and $T_c \sim 10.5$ K for $x=0.175$, respectively. The relatively sharp transition to superconducting state observed in the transport measurements indicates homogeneous superconducting properties in the films. The highest T_c^0 values were obtained for $x=0.15$, which corresponds with the expected 0.15 electrons/ CuO_2 for optimum doping. This is in contrast with the results presented to date in literature on the $\text{Sr}_{1-x}\text{La}_x\text{CuO}_2$ system, where the highest T_c was observed for $x=0.10$.⁶ The electrical properties of the films grown on $\text{BaTiO}_3/\text{SrTiO}_3$ [Fig. 3(b)] indicate that they are insufficiently electron doped, probably due to incomplete relaxation of the buffer layer. As a result, the BaTiO_3 layer does not provide sufficient tensile strain in order to promote adequate electron doping.¹³ Superconductivity with a reduced T_c^0 value of ~ 10 K was observed for some $x=0.15$ films grown on $\text{BaTiO}_3/\text{SrTiO}_3$ [the $0.15^\#$ film in Fig. 3(b)] only when the buffer layer was relaxed by annealing in vacuum (2 h at 900°C and 5×10^{-7} mbar) prior to the deposition of the $\text{Sr}_{1-x}\text{La}_x\text{CuO}_{2-\delta}$ film. Presence of local cation deficiency at the Sr(La) site, as detected by XRF analysis, is another possible reason for lack of superconductivity in these films.⁵ It is worth noting that an onset of superconductivity at ~ 22 K (no zero resistance at 4.2 K) was observed for some $x=0.10$ and $x=0.125$ films containing $(\text{Sr}, \text{La})_{14}\text{Cu}_{24}\text{O}_{41-\delta}$ as impurity phase.

Based on the transport measurements, some observations can be made: (i) the absence of the underdoped superconducting region, (ii) a narrow La doping range for superconductivity, with onset at $x=0.15$ and a subsequent disappearance of superconductivity for $x > 0.175$ with increasing concentration of electrons, and (iii) shift of the superconducting region toward a higher La doping level as compared to previous studies. Similar behavior has been reported in other electron-doped high- T_c systems, e.g., $\text{Nd}_{2-x}\text{Ce}_x\text{CuO}_4$,¹⁴ but not in the $\text{Sr}_{1-x}\text{La}_x\text{CuO}_2$ system. A reason for the observed shift in the electronic phase diagram may be the presence of oxygen vacancies in the Cu–O planes that may generate excess charge carriers. The data presented here also suggest that the range of La doping where superconductivity is present in $\text{Sr}_{1-x}\text{La}_x\text{CuO}_2$ may be wider than previously reported.

In summary, single-phase $\text{Sr}_{1-x}\text{La}_x\text{CuO}_2$ thin films with an IL-type structure were grown by PLD on KTaO_3 and SrTiO_3 substrates, both buffered with BaTiO_3 . The IL phase is obtained after oxidation of the as-deposited oxygen-deficient $\text{Sr}_{1-x}\text{La}_x\text{CuO}_{2-\delta}$ films having a $2\sqrt{2}a_p \times 2\sqrt{2}a_p \times c$ structure. An increased stability of the IL- $\text{Sr}_{1-x}\text{La}_x\text{CuO}_2$ phases for La doping levels up to $x=0.20$ as well as a modified and narrower doping range for superconductivity (i.e., for $0.15 \leq x \leq 0.175$) were observed. The $x=0.15$ films showed the optimum doping with a maximum T_c of 16 K. Improvement of the cooling procedure and therefore of the oxygen network may result in better superconducting properties. The presented synthesis method enables the epitaxial growth of all IL superconducting heterostructures such as superconductor–normal metal–superconductor Josephson junctions.

The financial support of the Dutch Science Foundation (FOM) is acknowledged. One of the authors (S.B.) is grateful to the Fund of Scientific Research-Flanders.

- ¹M. G. Smith, A. Manthiram, J. Zhou, J. B. Goodenough, and J. T. Markert, *Nature (London)* **351**, 549 (1991).
- ²G. Er, S. Kikkawa, F. Kanamaru, Y. Miyamoto, S. Tanaka, M. Sera, M. Sato, Z. Hiroi, M. Takano, and Y. Bando, *Physica C* **196**, 271 (1992).
- ³N. Ikeda, Z. Hiroi, M. Azuma, M. Takano, Y. Bando, and Y. Takeda, *Physica C* **210**, 367 (1993).
- ⁴H. Adachi, T. Satho, Y. Ichikawa, K. Setsune, and K. Wasa, *Physica C* **196**, 14 (1992).
- ⁵N. Sugii, H. Yamauchi, and M. Izumi, *Phys. Rev. B* **50**, 9503 (1994).
- ⁶ KTaO_3 substrates were used before with success for growing superconducting $\text{Sr}_{1-x}\text{La}_x\text{CuO}_2$ films by means of molecular beam epitaxy, see S. Karimoto, K. Ueda, M. Naito, and T. Imai, *Appl. Phys. Lett.* **79**, 2767 (2001).
- ⁷M. R. Presland, J. L. Tallon, R. G. Buckley, R. S. Liu, and N. E. Flower, *Physica C* **176**, 95 (1991).
- ⁸See, e.g., B. Mercey, A. Gupta, M. Hervieu, and B. Raveau, *J. Solid State Chem.* **116**, 300 (1995) and references therein.
- ⁹S. Bals, G. van Tendeloo, G. Rijnders, M. Huijben, V. Leca, and D. H. A. Blank, *IEEE Trans. Appl. Supercond.* **13**, 2834 (2003).
- ¹⁰V. Leca, Ph.D. thesis, University of Twente, 2003.
- ¹¹A. J. H. M. Rijnders, G. Koster, D. H. A. Blank, and H. Rogalla, *Appl. Phys. Lett.* **70**, 1888 (1997).
- ¹²The in-plane cell parameters for bulk KTaO_3 and BaTiO_3 are 3.989 and 4.02 Å, respectively. For SrTiO_3 , $a=3.905$ Å.
- ¹³J. T. Markert, T. C. Messina, B. Dam, J. M. Huijbreghse, J. H. Rector, and R. Griessen, *Proc. SPIE* **4058**, 141 (2000).
- ¹⁴H. Takagi, S. Uchida, and Y. Tokura, *Phys. Rev. Lett.* **62**, 1197 (1989).